Proceedings of the ASME 2018 Dynamic Systems and Control Conference
DSCC2018
September 30-October 3, 2018, Atlanta, Georgia, USA

DSCC2018-9157

SEMI-ACTIVE CONTROL FOR TWO-BODY OCEAN WAVE ENERGY CONVERTER BY USING HYBRID MODEL PREDICTIVE CONTROL

Qiuchi Xiong, Xiaofan Li, Dillon Martin, Sijing Guo, Lei Zuo
Department of Mechanical Engineering
Virginia Polytechnic Institute and State University, Blacksburg, VA, 24061
*Email: leizuo@vt.edu

ABSTRACT

Model predictive control (MPC) has been considered as one important feed-forward optimal control strategy for ocean wave energy converter (WEC) targeted on power maximization. The capability of MPC to handle system constraints (ex. stroke, velocity, actuator limitations), and the availability to provide optimal solution for linear system provide potential for the implementation of such algorithm in the WEC control. However, currently, only active MPC control has been introduced for single and two-body WECs. Such control strategy may introduce negative power during the optimization process, since the power take-off (PTO) damping has no constraint. In this paper, we proposed a hybrid MPC strategy in limiting both the PTO damping force and PTO damping to avoid negative power generation during cost function minimization (negative power minimization) for the two-body WEC. The problem is formulated into a quadratic programming (QP) problem targeted at power maximization. However, the standard QP problem formulation cannot be directly applied to the semi-active control problem due to the PTO damping constraints. Therefore, the problem is reformulated as a Mixed-integer Quadratic Programming (MIQP) problem, which contains logical switch to select constraint matrices based on the sign of the relative velocity between the buoy and submerged body. The optimal solution is compared with those of the active MPC control strategy and the passive model with the same irregular wave input.

1 INTRODUCTION

The energy from ocean wave is the most conspicuous form of ocean energy. The possibility of converting wave energy into usable energy has inspired numerous inventors. The major wave energy converter can be categorized into three types: oscillating water column (OWC), oscillating body, and overtopping systems [1]. Point absorber, one type of oscillating body, becomes popular due to its capability to absorb energy from waves in different directions. The simplest point absorber is the heaving buoy reacting against a fixed frame of reference (the sea level). The first development of such device can be dated back to 1980, which was tested in Tokyo Bay [2]. However, compared to the higher natural frequency of the point absorber (due to size limitation), the majority of energy in waves exists at low frequencies, which results in low energy harvesting efficiency. Therefore, two-body WEC system which includes a submerged second body has been developed to expand the power band of the device [3].

Based on the vibration theory, the majority of power produced by WEC devices occurs during resonant absorption when the wave excitation force is in phase with the device velocity [4]. Ocean wave is a wave spectrum consists of multiple frequencies and amplitudes. Therefore, control of WEC system becomes inevitable to let device velocity match with the input excitation force in time to maximize energy extraction. Based on the velocity matching theory, several sub-optimal and optimal control strategies have been developed. Starting from the single frequency wave WEC control, Budai and Fanes [5] introduced reactive control in the early 1970s according to the matching of the PTO damping to the impedance of the system transfer function from excitation force to device velocity. Such control strategies can only have good performance in regular wave case and cannot be applied with PTO load limitation, which makes it a type of sub-optimal strategy. The application of reactive control or similar strategies has not been applied to two body system due to more complicated system dynamics.

With the consideration of energy maximization among a power band with frequency spectrum, time domain optimal control can be a better way to maximize power absorption at each time point. However, in practice, most WECs will be subjected to limitations placed on physical motion of the absorber and the capabilities. Hence, it is necessary to develop constrained optimal control. In such a category of approach, model predictive control (MPC) becomes more and more attractive due to its capability in handling hard constraints on states and inputs, which serves the objective to maximize energy extraction and satisfies machinery requirements for safety and operations [6,7,8]. The MPC algorithm optimizes a cost function by predicting system future states within a pre-defined time horizon. Therefore, a prediction of wave behavior is necessary to assure perfect state prediction for optimization. In our case, we assume the full knowledge of wave is available within the prediction horizon.

Within current application, various methods were proposed to implement MPC on linear and nonlinear systems. One popular approach is to form the optimization problem into a Quadratic Programming (QP) form to efficiently calculate the convex problem [9]. In the thesis of Markus [10], he introduced the QP formulation for single-body and two-body WEC systems with the control input as the generator force. He showed that MPC is a very promising and adequate approach to control point absorber WEC. However, a negative power generation during the control period will occur with active WEC control. Shangyan [11] proposed a nonlinear MPC strategy on a single-body point absorber with the consideration of 3-DOF motion (surge, pitch, heave), which shows the consideration of 3-DOF motion can absorb more than three times energy compared to that of the system only considers heave motion. Qian [6], also developed an efficient convex MPC control strategy with control force limitation for WEC system to ensure control feasibility and improve computational efficiency.

Based on the knowledge of the authors of the paper, the MPC algorithm has been applied to both single-body and two-body linear and nonlinear systems. However, the negative power generation problem arisen by active constraints on PTO force has not been solved in current applications. As for point absorber, several PTO design concepts have been developed (ex. hydraulic, linear generator, turbine). Linear generator has been identified as one promising way to directly convert heave motion of the buoy into electricity due to high efficiency in mechanical gear system [1]. Such device can have a changeable external resistor acting as the actuator to vary PTO damping. Therefore, the system cannot provide a negative PTO damping and has an upper bound in it as well. The limitation of PTO damping value has the capability to avoid negative power generation. However, a control strategy that can consider the damping limitation should be addressed. We proposed a hybrid model predictive (HMPC) semi-active control strategy, which includes the PTO damping constraints as well as switch logic depending on the sign of relative velocity between the buoy and the submerged body for a two-body WEC system. The system is modeled into linear state-space model with the added mass and radiation damping generated from the boundary element condition software, WAMIT. The result of the HMPC is compared with that of a standard active MPC strategy. From the result, the semi-active control strategy successfully avoided the occurrence of negative power fed from the PTO to the buoy and the submerged body. The semi-active controller constrained the PTO damping to 12% of that of the active system with only 14% power loss. It successfully ensures safer PTO control operation and can have possibility to be applied into the PTO system with linear generator.

The paper is organized in the following format. Section 2 specifies the system modeling and problem formulation for active constrained optimal control problem. Section 3 specifies the problem formulation of hybrid MPC problem for semi-active control. Section 4 provides numerical simulation results and comparison among the active, semi-active control problems and the passive model. The conclusion is provided in section 5.

2 SYSTEM DYNAMIC MODELING AND THE FORMULATION OF ACTIVE MPC PROBLEM

In this section, the linear state-space model for the two body WEC system will be provided. A standard active MPC control strategy formulated into quadratic programming problem is introduced as the base system for comparison.

2.1 Modeling of Two Body WEC System

2.1.1 Equation of motion

Much work has already been done on the modeling of two-body point absorbers. In this paper, the modeling follows the work of Eidsmoen [12] and Ruehl. As show in the right figure in Figure 1, the buoy will be excited by the incident wave. Due to different excitation forces applied on the buoy and the submerged body, the relative motion of the buoy and the submerged body will drive the PTO system to rotate and generate electricity.

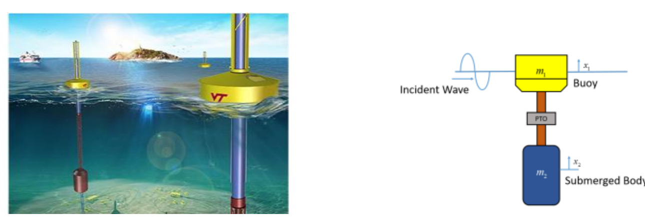

Figure 1. Two-body WEC [14] (left) and Schematic Diagram (right)

With the purpose to derive linear model for the two-body system, some assumptions need to be made:

1. The formulation is based on Linear Wave Theory (LTW).
2. Frequency dependent parameters of the two-body WEC are assumed to be constant.
3. The radiation forces are assumed to be linear and no convolution terms are used to calculate them.
4. Nonlinear viscous drag force is ignored for both buoy and submerged body.

In the schematic diagram in Figure 1, x_1, x_2 represent the position of the buoy and the submerged body. Based on

Newton's law, the dynamic equation of the buoy can be written as:

$$F_{gen} + F_{e1} - F_{r1} - F_{h1} - F_{r12} = m_1 \ddot{x}_1 \tag{1}$$

where $\ddot{x}_1$ is the buoy acceleration, m_1 is the mass of the buoy, F_{gen} is the force produced by the PTO system, F_{r_1} is the radiation damping force of the buoy, F_{r12} is the radiation damping force on the buoy generated by the submerged body motion, F_{h1} is the buoy hydrostatic force, and F_{e1} is the wave excitation force encountered by the buoy. The radiation force has been modeled as the combination of the buoy added mass as well as the radiation damping force. The hydrostatic force is modeled as linear force respect to the buoy position. The forces are:

$$F_{r1} = A_1 \ddot{x}_1(t) + b_1 \dot{x}_1(t) \tag{2}$$

$$F_{r12} = A_{12} \ddot{x}_2(t) \tag{3}$$

$$F_{h1} = \rho g \pi r_{buoy}^2 x_1(t) = k_1 x_1(t) \tag{4}$$

where A_1 is the buoy added mass, A_{12} is the buoy added mass due to the motion of the submerged body, b_1 is the buoy radiation damping, b_{12} should be the buoy radiation damping due to the motion of the submerged body. In the simulation, we assume the distance between the buoy and submerged body is long enough to ignore the radiation damping due to relative motion. The added mass and radiation damping are generated by WAMIT and are related to frequency. For simplification, they are assumed as constants at infinite frequency. Same assumption is also valid for submerged body. ρ is the water density, r_{buoy} is the radius of the buoy cross-section, g is the gravitational acceleration. $\rho g \pi r_{buoy}^2$ can be formed as a single variable k_1, the hydrostatic stiffness.

The same procedure can be applied to the submerged body. It follows that:

$$-F_{gen} + F_{e2} - F_{r2} - F_{r21} = m_2 \ddot{x}_2 \tag{5}$$

$$F_{r2} = A_2 \ddot{x}_2 + b_2 \dot{x}_2 \tag{6}$$

$$F_{r21} = A_{21} \ddot{x}_1 \tag{7}$$

The buoyancy force is constant due to fully submerge of the body. We assume the buoyancy force can be countered by a mooring force.

2.1.2 State-space formulation and discretization

With the purpose to control the system via MPC, a discrete-time state-space representation is necessary. The formulation process is not straightforward, due to the coupling terms within the coupled radiation calculation. This coupling occurs in the second derivative; hence a state-space model cannot be formed without reformulating first. Equation (1)-(7) can be rewritten as:

$$\frac{F_{gen} + F_{e1} - b_1 \dot{x}_1 - k_1 x_1 - A_{12} \ddot{x}_2}{m_1 + A_1} = \ddot{x}_1 \tag{8}$$

$$\frac{-F_{gen} + F_{e2} - b_2 \dot{x}_2 - A_{21} \ddot{x}_1}{m_2 + A_2} = \ddot{x}_2 \tag{9}$$

By plugging (8) into (9) and vice versa to get rid of the coupling terms $A_{12} \ddot{x}_2$ and $A_{21} \ddot{x}_1$. The equation can be restated as:

$$\underbrace{(m_1 + A_1 - \frac{A_{12} A_{21}}{m_2 + A_2})}_{m_{e1}} \ddot{x}_1 = F_{gen} + F_{e1} - b_1 \dot{x}_1 - k_1 x_1 + \frac{A_{12}}{m_2 + A_2} F_{gen} - \frac{A_{12}}{m_2 + A_2} F_{e2} + \frac{A_{12} b_2}{m_2 + A_2} \dot{x}_2 \tag{10}$$

$$\underbrace{(m_2 + A_2 - \frac{A_{21} A_{12}}{m_1 + A_1})}_{m_{e2}} \ddot{x}_2 = -F_{gen} + F_{e2} - b_2 \dot{x}_2 - \frac{A_{21}}{m_1 + A_1} F_{gen} - \frac{A_{21}}{m_1 + A_1} F_{e1} + \frac{A_{21} b_1}{m_1 + A_1} \dot{x}_1 + \frac{A_{21} k_1}{m_1 + A_1} x_1 \tag{11}$$

The state vector $x = \begin{pmatrix} x_1 & \dot{x}_1 & x_2 & \dot{x}_2 \end{pmatrix}^T$ and the initial conditions $x_0 = \begin{pmatrix} 0 & 0 & 0 & 0 \end{pmatrix}^T$. The system state-space form is:

$$\begin{aligned} \dot{x} &= Ax + BF_{gen} + B_1 F_{e1} + B_2 F_{e2} \\ Y &= Cx \end{aligned} \tag{12}$$

where

$$A = \begin{pmatrix} 0 & 1 & 0 & 0 \\ -\frac{k_1}{m_{e1}} & -\frac{b_1}{m_{e1}} & 0 & \frac{A_{12} b_2}{m_{e1}(m_2 + A_2)} \\ 0 & 0 & 0 & 1 \\ \frac{A_{21} k_1}{m_{e2}(m_1 + A_1)} & \frac{A_{21} b_1}{m_{e2}(m_1 + A_1)} & 0 & -\frac{b_2}{m_{e2}} \end{pmatrix}, B = \begin{pmatrix} 0 \\ \frac{1}{m_{e1}} + \frac{A_{12}}{m_{e1}(m_2 + A_2)} \\ 0 \\ -\frac{1}{m_{e2}} - \frac{A_{21}}{m_{e2}(m_1 + A_1)} \end{pmatrix} \tag{13}$$

$$B_1 = \begin{pmatrix} 0 \\ \frac{1}{m_{e1}} \\ 0 \\ -\frac{A_{21}}{m_{e2}(m_1 + A_1)} \end{pmatrix}, B_2 = \begin{pmatrix} 0 \\ -\frac{A_{12}}{m_{e1}(m_2 + A_2)} \\ 0 \\ \frac{1}{m_{e2}} \end{pmatrix}, C = \begin{pmatrix} 1 & 0 & -1 & 0 \\ 0 & 1 & 0 & -1 \end{pmatrix} \tag{14}$$

In what follows, the inputs F_{gen}, F_{e1}, F_{e2} are denoted by u, v, w, respectively. Then, the state space model is discretized by "Zero Order Hold (ZOH)" with the sampling time T_s to obtain the following discrete-time model:

$$\begin{aligned} x_{k+1} &= A_d x_k + B_d u_k + B_{d1} v_k + B_{d2} w_k, \qquad x_0 \in \mathbb{R}^4 \\ y_k &= C_d x_k \end{aligned} \tag{15}$$

where

$$A_d = e^{AT_s}, B_d = \int_0^{T_s} e^{A\tau} d\tau B, B_{d1} = \int_0^{T_s} e^{A\tau} d\tau B_{d1}, B_{d2} = \int_0^{T_s} e^{A\tau} d\tau B_{d2}, C_d = C \tag{16}$$

2.2 Active MPC Formulation

For the single body WEC, a reference buoy velocity can be calculated based on the transfer function from the wave excitation force to the buoy velocity. However, for two body system, there is no information about an optimal velocity trajectory. Therefore, the MPC is formulated with the purpose to directly maximize power extraction.

The optimization problem for the two-body WEC can be defined as:

$$\min_{x_k, u_k} \ J(x_k, u_k) \tag{17}$$

where

$$J(x_k,u_k) = -\sum_{k=1}^{N}[-q\underbrace{(\dot{x}_{1(k)}-\dot{x}_{2(k)})u_k}_{-P_{gen}} - ru_k^2] \tag{18}$$

subject to

$$x_{k+1} = A_d x_k + B_d u_k + B_{d1} v_k + B_{d2} w_k \tag{19}$$

$$\Delta x_{\min} \le x_{1(k+1)} - x_{2(k+1)} \le \Delta x_{\max}, \forall k = 1,...,N \tag{20}$$

$$\Delta \dot{x}_{\min} \le \dot{x}_{1(k+1)} - \dot{x}_{2(k+1)} \le \Delta \dot{x}_{\max}, \forall k = 1,...,N \tag{21}$$

$$u_{\min} \le u_k \le u_{\max}, \forall k = 0,..., N-1 \tag{22}$$

The problem has the constraints on relative position (stroke length) and velocity between the buoy and the submerged body. There are also constraints on the generator force.

The vector of the predicted states, control input and excitation forces are formulated as:

$$X = \left(x_1^T \quad x_2^T \quad \cdots \quad x_N^T\right)^T, U = \left(u_0 \quad u_1 \quad \cdots \quad u_{N-1}\right)^T \tag{23}$$
$$V = \left(v_0 \quad v_1 \quad \cdots \quad v_{N-1}\right)^T, W = \left(w_0 \quad w_1 \quad \cdots \quad w_{N-1}\right)^T$$

Solving system (19) and substituting in itself yields:

$$X = J_x x_0 + J_u U + J_v V + J_w W \tag{24}$$

where

$$J_x = \begin{pmatrix} A_d \\ A_d^2 \\ \vdots \\ A_d^N \end{pmatrix}, J_u = \begin{pmatrix} B_d & 0 & 0 & \cdots & 0 \\ A_d B_d & B_d & 0 & \cdots & 0 \\ A_d^2 B_d & A_d B_d & B_d & \cdots & 0 \\ \vdots & \vdots & \vdots & \ddots & \vdots \\ A_d^{N-1} B_d & A_d^{N-2} B_d & A_d^{N-3} B_d & \cdots & B_d \end{pmatrix} \tag{25}$$

$$J_{v(w)} = \begin{pmatrix} B_{d1(2)} & 0 & 0 & \cdots & 0 \\ A_d B_{d1(2)} & B_{d1(2)} & 0 & \cdots & 0 \\ A_d^2 B_{d1(2)} & A_d B_{d1(2)} & B_{d1(2)} & \cdots & 0 \\ \vdots & \vdots & \vdots & \ddots & \vdots \\ A_d^{N-1} B_{d1(2)} & A_d^{N-2} B_{d1(2)} & A_d^{N-3} B_{d1(2)} & \cdots & B_{d1(2)} \end{pmatrix} \tag{26}$$

and $\dim(J_u, J_v, J_w) = (4N \times N), \dim(J_x) = (4N \times 4)$ (27)

The objective function (18) can be reformulated as:

$$J(X,U) = q(X_{(2)} - X_{(4)})^T U + U^T \hat{R} U = q(S_1 X - S_2 X)^T U + U^T \hat{R} U = qX^T \underbrace{(S_1^T - S_2^T)}_{S} U + U^T \hat{R} U \tag{28}$$

with the matrix $\hat{R} = diag(r)$ with $\dim(\hat{R}) = (N \times N)$, and the matrices S_1, S_2 with $\dim(S_1, S_2) = (N \times 4N)$. S_1 and S_2 extract the second state (buoy velocity) and fourth state (submerged body velocity) from X.

$$S_1 = \begin{pmatrix} (0 \; 1 \; 0 \; 0) & \cdots & 0 \\ \vdots & \ddots & \vdots \\ 0 & \cdots & (0 \; 1 \; 0 \; 0) \end{pmatrix}, S_1 = \begin{pmatrix} (0 \; 0 \; 0 \; 1) & \cdots & 0 \\ \vdots & \ddots & \vdots \\ 0 & \cdots & (0 \; 0 \; 0 \; 1) \end{pmatrix} \tag{29}$$

By using (24), the objective function can be formulated as a quadratic function only depends on U.

$$J(U) = \frac{1}{2} U^T \underbrace{(qJ_u^T S + \hat{R})}_{H} U + \underbrace{q(x_0^T J_x^T + V^T J_v^T + W^T J_w^T) S}_{F^T} U \tag{30}$$

where H is the Hessian matrix. It is positive semi-definite (PSD) to ensure the QP problem to be a convex problem with available solution.

The constraints can also be augmented respect to U. Therefore, the active MPC can be written as:

$$\min_U J(U) = J(U) = \frac{1}{2} U^T (qJ_u^T S + \hat{R}) U + q(x_0^T J_x^T + V^T J_v^T + W^T J_w^T) SU \tag{31}$$

subject to

$$\begin{pmatrix} D_D \\ E_D J_u \end{pmatrix} U \le \begin{pmatrix} \underline{d} \\ \underline{e} - E_D J_x x_0 - E_D J_v V - E_D J_w W \end{pmatrix} \tag{32}$$

The active MPC problem is a standard quadratic programming problem, hence can be solved efficiently by the "quadprog" command in MATLAB.

3 HYBRID MPC FORMULATION FOR SEMI-ACTIVE DAMPING CONTROL

In this section, the formulation of the semi-active PTO damping control will be introduced with the formulation of a hybrid MPC. The PTO damping is calculated as:

$$C_{pto} = \frac{-F_{gen}}{\dot{x}_1 - \dot{x}_2} \tag{33}$$

where F_{gen} is the generator force and the $\dot{x}_1 - \dot{x}_2$ is the relative velocity between the buoy and the submerged body. The negative sign is used to represent that the damping force is always in the negative direction compared to the relative velocity. If the sign of the generator force is the same as that of the relative velocity, a negative PTO damping will occur. In the active control problem, negative PTO damping may appear to cause negative generated power. It is obvious to see that PTO damping is generated by a nonlinear equation because both relative velocity and generator force are changing variables. To simplify the problem, a linear representation of the C_{pto} is defined here. The Hybrid System Descriptive Language (HYSDEL) software tool is used to define the HMPC problem [15]. The HYSDEL is a high-level descriptive language used to describe a hybrid dynamic system. It can directly describe the formulation of the hybrid MPC system for the semi-active damping control for two-body WEC.

3.1 Linear Representation of C_{pto}

The generator force can be re-written as:

$$F_{gen} = -C_{pass}(\dot{x}_1 - \dot{x}_2) + u = C_{pto}(\dot{x}_1 - \dot{x}_2) = (-C_{pass} + C_u)(\dot{x}_1 - \dot{x}_2) \tag{34}$$

where $C_{pass} = \frac{C_{\max} + C_{\min}}{2}$ [20], u is the damping force input, C_u is the PTO damping for u, $C_{\max}$ and $C_{\min}$ are the maximum and minimum PTO damping a system can achieve. The reason to choose C_{pass} to be the average value of $C_{\max}$ and $C_{\min}$ is to determine a damping value for the passive model. Then, the HMPC algorithm will search for optimal control force that results in a damping variation around the passive system damping. Based on the modification, the generator (damping) force limitation can be expressed as:

$$-C_{\max}(\dot{x}_1-\dot{x}_2)\le -C_{pass}(\dot{x}_1-\dot{x}_2)+u\le -C_{\min}(\dot{x}_1-\dot{x}_2),\ \text{if}\ \ \dot{x}_1-\dot{x}_2\ge 0 \quad (35)$$

$$-C_{\min}(\dot{x}_1-\dot{x}_2)\le -C_{pass}(\dot{x}_1-\dot{x}_2)+u\le -C_{\max}(\dot{x}_1-\dot{x}_2),\ \text{if}\ \ \dot{x}_1-\dot{x}_2< 0$$

From the equation (35), the constraints for u respect to PTO damping have been converted into linear inequality equations. However, the constraints depend on the sign of the relative velocity, which means a hybrid MPC [16] needs to be applied.

Since the generator force consists of both control force and damping force generated by C_{pass}, with the purpose to be compared to active control, the limitation on the generator force is same for the semi-active control problem, which will result in a different force limitation on u. The force constraint can be rewritten as:

$$u_{\min}\le F_{gen}\le u_{\max}\Rightarrow u_{\min}\le -C_{pass}(\dot{x}_1-\dot{x}_2)+u\le u_{\max} \quad (36)$$

where $u_{\max}, u_{\min}$ are the same parameters with same values in the active control problem.

3.2 Hybrid MPC Formulation

3.2.1 Cost function modification

Since the control force u has been modified as part of the generator force due to linear representation of PTO damping constraints, the extracted power can be written as:

$$P_{gen}=-F_{gen}(\dot{x}_1-\dot{x}_2)=-(u-C_{pass}(\dot{x}_1-\dot{x}_2))(\dot{x}_1-\dot{x}_2)=C_{pass}(\dot{x}_1-\dot{x}_2)^2-u(\dot{x}_1-\dot{x}_2) \quad (37)$$

Therefore, based on the P_{gen}, the cost function can be reformulated as:

$$J(x_k,u_k)=-\sum_{k=1}^{N}[-q(\underbrace{-C_{pass}(\dot{x}_{1(k)}-\dot{x}_{2(k)})^2+u_k(\dot{x}_{1(k)}-\dot{x}_{2(k)})}_{-P_{gen}})-ru_k^2] \quad (38)$$

3.2.2 Constraints and MPC problem formulation

First, we need to define the polyhedron regions the problem will be solved. We have constraints on input force u, PTO damping. The state constraints will not change for semi-active MPC.

$$\text{Polyhedron 1:}\ \begin{cases} u\le 0 \\ -u+C_{pass}(\dot{x}_1-\dot{x}_2)\le -u_{\min} \\ -u+\dfrac{C_{\min}-C_{\max}}{2}(\dot{x}_1-\dot{x}_2)\le 0 \\ u+\dfrac{C_{\min}-C_{\max}}{2}(\dot{x}_1-\dot{x}_2)\le 0 \end{cases},\ \text{if}\ \ \dot{x}_1-\dot{x}_2\ge 0 \quad (39)$$

$$\text{Polyhedron 2:}\ \begin{cases} -u\le 0 \\ u-C_{pass}(\dot{x}_1-\dot{x}_2)\le u_{\max} \\ -u+\dfrac{C_{\max}-C_{\min}}{2}(\dot{x}_1-\dot{x}_2)\le 0 \\ u+\dfrac{C_{\max}-C_{\min}}{2}(\dot{x}_1-\dot{x}_2)\le 0 \end{cases},\ \text{if}\ \ \dot{x}_1-\dot{x}_2< 0 \quad (40)$$

We can consider a logic binary variable $\delta_s=\begin{pmatrix}0 & 1\end{pmatrix}^T$. $\delta_s=1\rightarrow \dot{x}_1-\dot{x}_2\ge 0, \delta_s=0\rightarrow \dot{x}_1-\dot{x}_2<0$.

By defining variable $z_s, z_c, z_{bound}\le 0$ as:

$$z_s=\begin{cases} u, & \delta_s=1 \\ -u, & \delta_s=0 \end{cases},\quad z_c=\begin{cases} \begin{pmatrix} -u+\dfrac{C_{\min}-C_{\max}}{2}(\dot{x}_1-\dot{x}_2) \\ u+\dfrac{C_{\min}-C_{\max}}{2}(\dot{x}_1-\dot{x}_2)\end{pmatrix}, & \delta_s=1 \\ \begin{pmatrix} -u+\dfrac{C_{\max}-C_{\min}}{2}(\dot{x}_1-\dot{x}_2) \\ u+\dfrac{C_{\max}-C_{\min}}{2}(\dot{x}_1-\dot{x}_2)\end{pmatrix}, & \delta_s=0 \end{cases} \quad (41)$$

$$z_{bound}=\begin{cases} -u+C_{pass}(\dot{x}_1-\dot{x}_2)+u_{\min}, & \delta_s=1 \\ u-C_{pass}(\dot{x}_1-\dot{x}_2)-u_{\max}, & \delta_s=0 \end{cases} \quad (42)$$

The input constraints combined with the original dynamic system can be formulated as a mixed logical dynamic system (MLD) [17] for controller design.

$$\begin{aligned} x_{k+1}&=A_d x_k+B_d u_k+B_{d1}v_k+B_{d2}w_k+B_1\delta_{s-k}+B_2 z_k \\ E_2\delta_{s-k}&+E_3 z_k\le E_1 u_k+E_4 x_k+E_5 \end{aligned} \quad (43)$$

where x_k, u_k, v_k, w_k are state variables, semi-active control force, buoy excitation force and submerged body excitation force at current time step k. δ_{s-k} is δ_s at time step k. $z_k=\begin{pmatrix}z_s & z_c & z_{bound}\end{pmatrix}^T$ are the auxiliary binary and continuous variables at time step k. A_d, B_d, B_{d1}, B_{d2} are discretized system matrices from the original state-space model in (15). The sampling time is T_s. The matrices $B_1, B_2, E_1, E_2, E_3, E_4, E_5$ are calculated automatically by the Multi Parametric Toolbox (MPT) [15] according to the descriptive HYSDEL language.

Based on the hybrid logic constraints, the hybrid MPC can be formulated as:

$$J(x_k,u_k)=-\sum_{k=1}^{N}[-q(-C_{pass}(\dot{x}_{1(k)}-\dot{x}_{2(k)})^2+u_k(\dot{x}_{1(k)}-\dot{x}_{2(k)}))-ru_k^2] \quad (44)$$

subject to

$$\begin{cases} x_{k+1}=A_d x_k+B_d[u_k-C_{pass}(x_{2(k)}-x_{4(k)})]+B_{d1}v_k+B_{d2}w_k+B_1\delta_{s-k}+B_2 z_k \\ E_2\delta_{s-k}+E_3 z_k\le E_1 u_k+E_4 x_k+E_5 \\ \Delta x_{\min}\le x_{1(k+1)}-x_{3(k+1)}\le \Delta x_{\max} \\ \Delta\dot{x}_{\min}\le x_{2(k+1)}-x_{4(k+1)}\le \Delta\dot{x}_{\max} \end{cases} \quad (45)$$

The procedure is to write the HYSDEL code, then convert the code as a MPT structure system into MATLAB. Since the system has measurable disturbances v, w, the YALMIP [18] toolbox inside the MPT toolbox is applied to manually input disturbance prediction according to simulation time step. The YALMIP toolbox has the flexibility to customize cost function. Finally, using the external called solver GUROBI [19], that contains the capability to solve MIQP problem, to optimize the problem based on user-defined cost function. The GUROBI solver has the capability to directly solve nonlinear cost function defined as in the problem.

4 CASE STUDY AND SIMULATION RESULT

4.1 Parameters and Inputs

4.1.1 Parameters

In this section, a set of parameters from a paper is applied as the dimensions and some properties of the two-body system.

The active and semi-active control law uses same parameters with same adjusted weights for states and control inputs. The active control simulation is implemented in the Simulink environment. The semi-active control simulation is implemented with MATLAB code. Table below shows the parameters used in both simulations.

Parameters	
Buoy mass [kg]	2625.3
Submerged body mass [kg]	2650.4
Buoy added mass [kg]	8866.7
Submerged body added mass [kg]	361.99
Buoy added mass due to submerged body [kg]	361.99
Submerged body added mass due to buoy [kg]	361.99
Buoy radiation damping [Ns/m]	5000
Submerged body radiation damping [Ns/m]	50000
Buoy hydrostatic stiffness [N/m]	96743
Sampling time [s]	0.1
Prediction step	100
Weight on power generation	10e6
Control input weight	10e(-6)
Prediction horizon [s]	10
Maximum generator force [N]	50000
Minimum generator force [N]	-50000
Maximum PTO damping [Ns/m]	20000
Minimum PTO damping [Ns/m]	0
Maximum stroke length [m]	0.75
Minimum stroke length [m]	-0.75
Maximum relative velocity [m/s]	1
Minimum relative velocity [m/s]	-1
Passive model PTO damping [Ns/m]	10000

Table 1. Parameters of the System [10]

4.1.2 Wave input

The wave input is a superposition of three regular waves with different amplitudes, frequencies and phases. The excitation force amplitudes are obtained from the coefficients calculated from WAMIT. Since the distance between the buoy and the submerged body is assumed to be long enough, the surface wave motion cannot have large effect on the submerged body, which results in a much smaller excitation force on the submerged body. The wave parameters are displayed in Table 2. The wave excitation forces for buoy and the submerged body are displayed in Figure 2. From the plot, it can be shown that the combined wave has a period equal to 10 s .

Buoy	Wave 1	Wave 2	Wave 3
Excitation force amplitude (N)	6074.8	19624	48121
Frequency (rad / s)	2.4 π	3 π	4 π
Phase (rad)	-0.5 π	0	0.5 π
Submerged body	**Wave 1**	**Wave 2**	**Wave 3**
Excitation force amplitude (N)	100.5428	324.1803	324.1803
Frequency (rad / s)	2.4 π	3 π	4 π
Phase (rad)	-0.5 π	0	0.5 π

Table 2. Wave Parameters

Wave Excitation Force

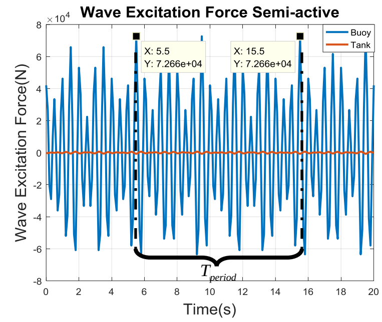

Figure 2. Wave Excitation Force Inputs for Buoy and the Submerged Body

4.2 Results Comparison and Discussion

Since the toolbox solver will need a long time to solve the problem in a standard desktop, the simulation time is set to 20s, which equals to two full periods of the input wave. The passive WEC model uses the constant PTO damping equals to C_{pass} in the simulation. The results of the relative position, relative velocity between the buoy and the submerged body for semi-active, active and passive systems are displayed in Figure 3. The relative velocity is also plotted with the excitation force applied on the WEC in Figure 4. The generator forces for semi-active, active, and passive systems are displayed in Figure 5. The resulting PTO damping for three cases are displayed in Figure 6 based on the calculation $C_{PTO} = F_{gen} / (\dot{x}_1 - \dot{x}_2)$. The PTO damping for semi-active control is displayed in Figure 7. The generated power for the semi-active, active and passive models are displayed in Figure 8.

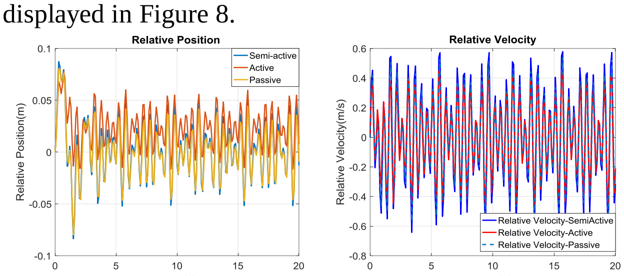

Figure 3. Buoy and Submerged Body Relative Position (Left) and Velocity (Right)

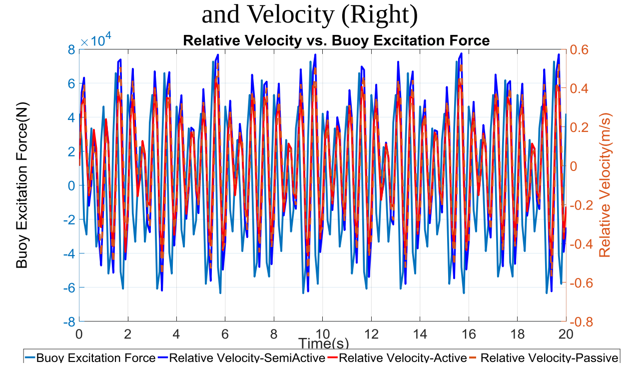

Figure 4. Relative Velocity and Wave Excitation on the WEC

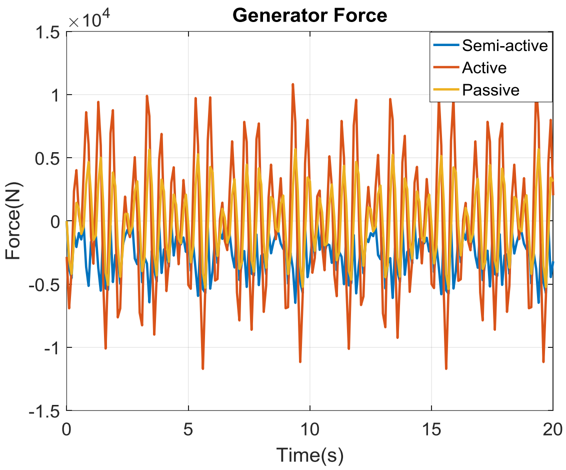

Figure 5. Generator Force for the WEC

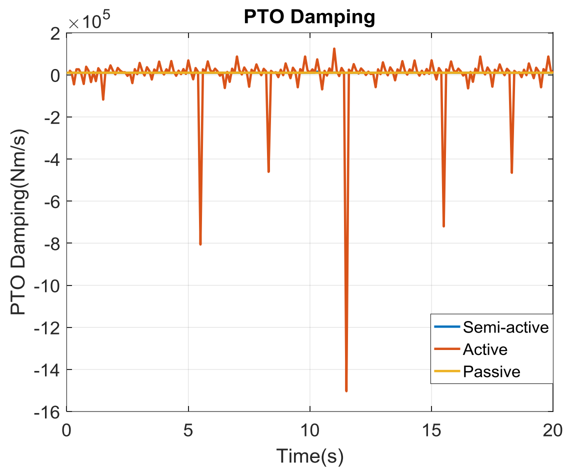

Figure 6. PTO Damping Comparison

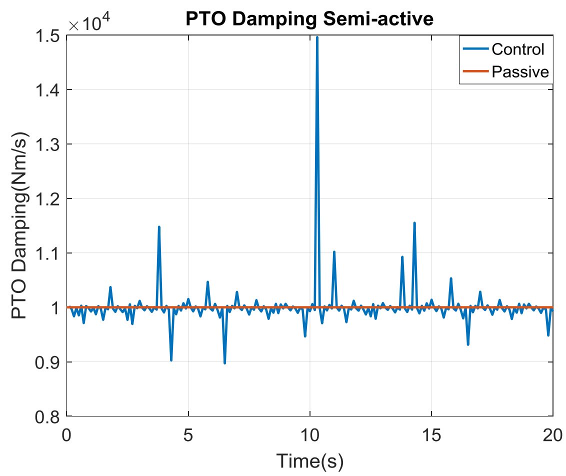

Figure 7 PTO Damping Comparison between Semi-active & Passive

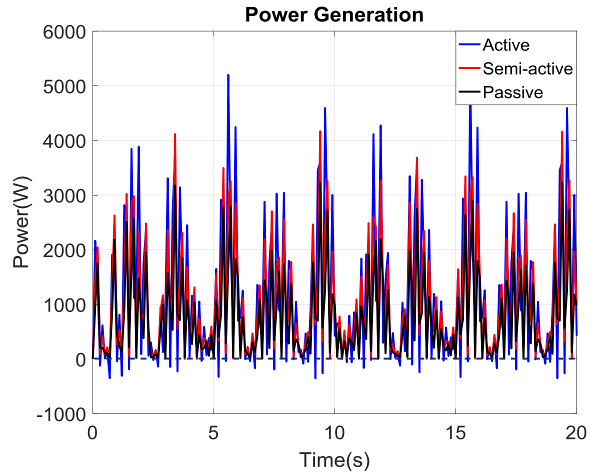

Figure 8. Power Generation Comparison

The relative position is set to be $-0.75 \le \Delta x \le 0.75$; the relative velocity is set to be $-1 \le \Delta \dot{x} \le 1$; the generator force is set to be $-50000 \le F_{gen} \le 50000$ for both semi-active and active systems. From Figure 3 and 5, the corresponding variables are within the pre-defined boundaries. By comparing Figure 6 and 7, the PTO damping for the active system (peak value can be $1.5 \cdot 10^6\, N \cdot m/s$) is much larger compared to that of semi-active (peak value is only $1.5 \cdot 10^4\, N \cdot m/s$) and passive systems ($1 \cdot 10^4\, N \cdot m/s$). Besides, the active PTO damping changes from positive value to negative value frequently. However, the PTO damping for semi-active system is constrained within the pre-defined damping constraint $0 \le C_{gen} \le 20000$. Since the damping value for the semi-active system is much smaller compared to that of the active system, the relative velocity becomes larger for semi-active system, which can be verified in Figure 3 on the right side. However, since the damping for semi-active system is much smaller compared to that of the active system and the relative velocity does not vary significantly for the active and semi-active systems, the generator force for the semi-active system is much smaller compared to that of the active and passive systems. The average damping for the three systems are analyzed as below:

As for the PTO damping for the semi-active system, it is always positive. Therefore, the average damping value is obtained by taking the root mean square of the PTO damping. As for the active system, the damping value changes between positive and negative values. Therefore, the average damping is calculated separately for positive and negative values. Then, the average PTO damping is calculated based on the summation average of the positive and negative damping values, which can be expressed as the equation below:

$$avg(C_{pto-active}) = \frac{rms(C_{pto-positive}) + rms(C_{pto-negative})}{2} \qquad (46)$$

where $rms(C_{pto-positive}), rms(C_{pto-negative})$ are the root mean square values for the positive and negative PTO damping values.

The damping suppression percentage from the semi-active system compared to that of the active system is calculated as:

$$P_{\text{suppresion}} \frac{avg(C_{pto-active}) - avg(C_{pto-semi-active})}{avg(C_{pto-active})} 100\% \quad (47)$$

where $avg(C_{pto-active})$, $avg(C_{pto-semi-active})$ are the average PTO damping for active and semi-active systems. The passive PTO damping is a constant. The resulting average PTO damping for the active, semi-active and passive systems are displayed in Table 3:

System	Average PTO Damping $(N \cdot s / m)$	Suppressing Percentage Respect to Active System (%)
Semi-active	9994	88
Active	84092	0
Passive	10000	N/A

Table 3. Average PTO Damping Comparison

Based on the theory, semi-active control will result in lower power extraction since system damping is restricted. From Figure 8, it is obvious to see that the power generation for semi-active system is less than that of the active system. From Figure 8, both semi-active and active systems can have larger generated power compared to that of the passive system, which shows the effectiveness of the controller. The average power for the three systems are calculated based on the equation as:

$$P_{avg} = \frac{1}{T}\int_0^T P_{gen} dt \quad (48)$$

where P_{gen} is the instant generator power, T is the simulation horizon (20s). The average power is the time integration of the generator power over the simulation horizon. The integration is calculated by the MATLAB command "trapz()". The calculated average power is displayed in Table 4. Power improvement percentage of semi-active and active systems respect to the passive model are also calculated in the Table 4. The power loss percentage of semi-active system compared to the power of the active system is calculated directly based on the power improvement percentage difference for those two systems.

System	Average Generated Power (W)	Power Improvement Percentage (%)
Semi-active	1033	35
Active	1139	49
Passive	763	0

From the table, it can be shown that the power loss for semi-active system is around 14% compared to that of the active system. The damping suppression effect for the semi-active system can be around 88% compared to that of the active system. The semi-active controller successfully considers both the generator force as well as the PTO damping which ensures safer operation for a PTO system in a WEC without sacrificing large amount of power generation

5 CONCLUSION

In this paper, a hybrid model predictive control (HMPC) strategy is applied on a two-body WEC targeted at power extraction maximization with the consideration of PTO damping (semi-active) as well as PTO force limitations. The two-body WEC system has been modeled as a linear time invariant state-space model by setting the frequency depend radiation damping as constant. A standard formulation of Quadratic Programming (QP) MPC has been applied with active control force on the WEC system as compared model. The HMPC has been formulated as a mixed integer quadratic programming (MIQP) problem and is solved by the MPT toolbox in MATLAB. The simulation result with same input parameters are analyzed and discussed for semi-active, active and passive cases. From the result, the semi-active controller has the ability to limit both the generator force and the PTO damping. The PTO damping control effort has been reduced by 88% compared to that of the active system with 14% of power loss. The controller displays the advantage in providing PTO with a safer operation condition and also provides the possibility to be applied to the PTO system with linear generator. As for WEC control, one major problem is the prediction of the wave. The current HMPC assumes a perfect prediction of the wave for at least one period, which is normally not possible in the real environment. Therefore, the future research topic can be addressed on the development of the wave estimator that can be combined with current MPC model. MPC is considered as a good optimal control strategy with large computational cost. From the simulation of the model in this paper, it takes 1.6 hours to generate results, which makes it hard in real time implementation. Therefore, the efficiency improvement of current algorithm can be another research topic in the future in algorithm optimization as well.

REFERENCES

[1] F. Antonio, "Wave energy utilization: A review of the technologies", *Renewable and Sustainable Energy Reviews*, 14, pp 899-918, 2010.

[2] Hirohisa T. "Sea trial of a heaving buoy wave power absorber". In: Berge H, editor. Proceedings of 2nd International Symposium on Wave Energy Utilization, Trondheim, Norway; 1982, p. 403–17.

[3] C. G. Ryan, B. Giorgio, "A comparison of control strategies for wave energy converters", *International Journal of Marine Energy*, 20, pp 45-63, 2017.

[4] W. David, B. Giorgio, "A comparison of WEC control strategies", Sandia National Lab Report, April, 2016.

[5] K. Budal, J. Falnes, Interacting point absorbers with controlled motion, in: B. Count (Ed.), *Power from Sea Waves*, Academic Press London, Edinburgh, Scotland, 1979, pp. 381–399.

[6] Z. Qian, Yeung. W. Ronald, "An efficient convex formulation for model-predictive control on wave-energy converter", *Journal of Offshore Mechanics and Arctic Engineering*, 140, June, 2018.

[7] Eidsmoen, H., 1996, “Optimum control of a floating wave-energy converter with restricted amplitude” *ASME J. Offshore Mech. Arct. Eng.*, 118(2), pp. 96–101.
[8] Evans, D., 1981, “Maximum wave-power absorption under motion constraints” *Appl. Ocean Res.*, 3(4), pp. 200–203.
[9] Hals, J., Falnes, J., and Moan, T., 2011, “Constrained optimal control of a heaving buoy wave-energy converter,” *ASME J. Offshore Mech. Arct. Eng*., 133(1), p. 011401.
[10] R. Markus, “Different model predictive control approaches for controlling point absorber wave energy converters”, University Stuttgart, Institute for System Dynamics, October, 2011.
[11] Z. Shangyan, A. Ossama, “Model predictive control of parametric excited pitch-surge modes in wave energy converter”, *International Journal of Marine Energy*, 19, 2017, pp 32-46.
[12] H. Eidsmoen. “Simulation of a slack-moored heaving-buoy wave-energy converter with phase control” PhD thesis, Norwegian University of Science and Technology, Trondheim, Norway, 1996.
[13] K. Ruehl, T. Brekken, B. Bosma, and R. Paasch, “Large-scale ocean wave energy plant modeling”, *Innovative Technologies for an Efficient and Reliable Electricity Supply (CITRES)*, 2010 IEEE Conference, pp 379 –386, September, 2010.
[14] “Ocean wave energy harvester using mechanical modified rectifier”, In the Virginia Tech Research Innovation Post, July, 2016, https://research.vt.edu/inventors-of-the-month/inventors-month-july-2016.
[15] M. Kvasnica, P. Grieder, and M. Baotic, MPT home page: http://control.ee.ethz.ch/~mpt/.
[16] Y. Liu, “Regenerative vibration control of tall buildings using model predictive control”, *Dynamic Systems and Control Conference (DSCC)*, 2013 ASME Conference.
[17] A. Bemporad and M. Morari, 1999. “Control of systems integrating logic, dynamics, and constraints,” *Automatica*, vol. 35, no. 3, pp. 407–427.
[18] J. Lofberg, YALMIP. [Online]. Available: http://users.isy.liu.se/johanl/yalmip/
[19] E. Rothberg, GUROBI home page: http://www.gurobi.com
[20] M. Nguyen, M. Canale, O. Sename, L. Dugard, “A Model Predictive approach for semi-active suspension control problem of a full car”, *55th IEEE Conference on Decision and Control (CDC 2016)*, Dec 2016, Las Vegas, United States. 2016. <hal-01361841